Imaging Techniques

DOI: 10.1002/ange.200904649

Multi-Frequency PARACEST Agents Based on Europium(III)-DOTA-Tetraamide Ligands**

*Subha Viswanathan, S. James Ratnakar, Kayla N. Green, Zoltan Kovacs, Luis M. De León-Rodríguez, and A. Dean Sherry**

Magnetic resonance imaging (MRI) is one of the most versatile and powerful diagnostic tools in modern medicine. Recently, a conceptually different approach to contrast enhancement based on chemical exchange saturation transfer (CEST) has emerged that takes advantage of slow-to-intermediate exchange conditions between two or more pools of protons ($k_{ex} \leq \Delta\omega$).[1] While the first reported CEST agents were diamagnetic molecules containing exchangeable NH and OH groups ($\Delta\omega \leq 5$ ppm), it was later shown that the slow water exchange characteristics of certain paramagnetic Ln^{3+} complexes of DOTA-tetraamide ligands allows selective saturation of a hyperfine shifted Ln^{3+}-bound water pool ($\Delta\omega > 50$ ppm) for creating CEST contrast.[2] Radio frequency (RF) saturation of highly shifted exchange resonances in paramagnetic systems offer significant advantages over diamagnetic CEST agents with small $\Delta\omega$ values.[3]

One of the primary advantages of CEST as a contrast mechanism is that the effect is detectable only when a RF pulse is applied at the specific frequency of the exchangeable protons. PARACEST (paramagnetic CEST) agents based on Ln^{3+} ions are particularly attractive in this respect because different ions across the lanthanide series can be used to prepare complexes with exchangeable protons covering a wide range of frequencies. The proof of principle for multi-frequency MRI was elegantly demonstrated by Aime and co-workers with Eu^{3+} and Tb^{3+}-based PARACEST agents.[4] "Multi-frequency" PARACEST agents such as these could be useful in imaging multiple biomarkers simultaneously since any parameter (pH, temperature, redox, metabolite concentration) that alters the water exchange kinetics will in turn alter image contrast.[5] To date, however, it has been largely the Eu^{3+} complexes that have displayed sufficiently slow water exchange kinetics to allow activation at sufficiently low RF power. Complexes of other lanthanide ions that induce large paramagnetic shifts (Tm^{3+}, Tb^{3+}, and Yb^{3+}) have faster than optimal water exchange kinetics and consequently their CEST detection sensitivities have been limited so far.[6] Although efforts to develop new ligands with optimal water exchange kinetics for these other more highly shifting lanthanide ions will likely continue, a more immediate approach would be to design a series of Eu^{III}-DOTA-tetraamide complexes for use as a "multi-frequency" imaging platform.

We have shown previously for Eu^{3+}-DOTA-tetraamide complexes that the nature of the extended amide side-chains (size, charge, and polarity) can have a significant effect on water exchange rates.[5c,7] It soon became apparent that the chemical shift of the bound water exchange peak in these complexes can also vary considerably by choosing an appropriate amino acid as the amide donor. We report here a series of multi-frequency Eu^{3+}-based PARACEST agents wherein each Eu^{3+} complex has a unique bound water resonance frequency. Most Eu^{3+}-based PARACEST agents reported to date have been based on the DOTA-$(gly)_4$ framework in which the bound water resonance is found around 50 ppm at room temperature.[6] In this work, we introduce three new Eu^{3+}-based complexes based on ligands **1**–**3** (Scheme 1; see also Schemes S1–S3 in the Supporting Information)[8] that show remarkably large differences in the resonance frequencies of the bound water protons.

In aqueous solution, Ln^{3+} complexes of DOTA-tetraamides exist in the form of two inter-converting coordination isomers—square anti-prism (SAP) and twisted square anti-prism (TSAP)—depending on the relative conformations of the amide side-arms and the macrocyclic ring. Interestingly, the two isomers always have markedly different water exchange rates, the TSAP isomer being considerably faster.[2,3,7a] As a result, CEST is typically observed for SAP isomers but not observed for TSAP isomers. Eu^{3+} complexes of DOTA-tetraamide ligands in which the amide functional groups are not sterically demanding are known to exist primarily as SAP structures, contributing to the slow water exchange kinetics found in these complexes.[2,7,9] High resolution ^{1}H NMR spectra of the three complexes (Figures S1–S3) indicate, as anticipated, that the complexes exist predominantly as SAP structures in solution. However, closer inspection of the most highly shifted axial ethylene protons of the cyclen ring, commonly referred to as the H4 protons (Figure S4) and located between 20 and 35 ppm in these

[*] Dr. S. Viswanathan, Dr. S. J. Ratnakar, Dr. K. N. Green, Prof. Z. Kovacs, Prof. L. M. De León-Rodríguez, Prof. A. D. Sherry
Advanced Imaging Research Center
University of Texas Southwestern Medical Center
5323 Harry Hines Boulevard, Dallas, Texas, 75390 (USA)
Fax: (+1) 214-645-2744
E-mail: dean.sherry@utsouthwestern.edu
Prof. A. D. Sherry
Department of Chemistry, University of Texas, Dallas
800 West Campbell Road, Richardson, Texas, 75080 (USA)

[**] The authors acknowledge financial support from the National Institutes of Health (CA-115531, CA-126608, RR-02584 and EB-004582) and the Robert A. Welch Foundation (AT-584) as well as the Deisenhofer Laboratory at UT Southwestern Medical Center for use of computational resources. DOTA = 1,4,7,10-tetraaza-1,4,7,10-tetrakis(carboxymethyl)cyclododecane.

Supporting information for this article is available on the WWW under http://dx.doi.org/10.1002/anie.200904649.

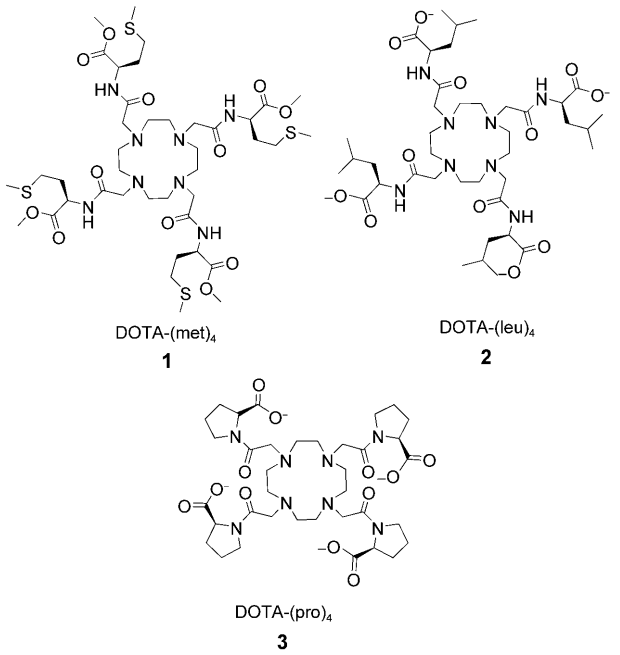

Scheme 1. DOTA tetraamide ligands studied in this work.

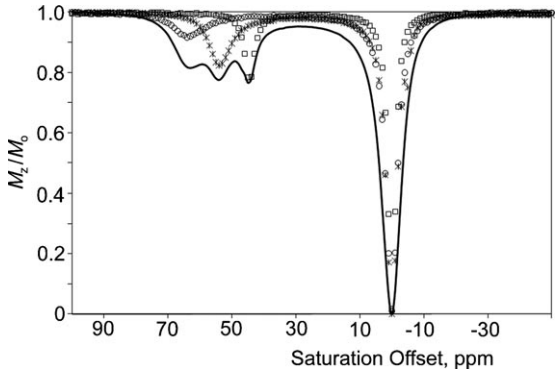

Figure 1. Individual CEST spectra for aqueous solutions of Eu-**1** (□, 20 mM) at 45 ppm, Eu-**2** (*, 15 mM) at 54 ppm, and Eu-**3** (○, 11 mM) at 64 ppm recorded at 9.4 T, 298 K, pH 7, $B_1 = 9.1\ \mu T$, and irradiation time of 5 s. The black trace shows the CEST spectrum of a mixture of all three complexes (each at 20 mM). M_z = net water magnetization at steady state in the presence of a presaturation pulse; M_0 = net water magnetization in the absence of a presaturation pulse.

complexes, revealed marked differences in the magnitude of the hyperfine shifts in this series. Interestingly, the chemical shift of H4 protons in Eu-**3** was surprisingly large compared to the other Eu^{III}-DOTA-tetraamide complexes (Table 1).

Table 1: Exchange lifetimes (τ_m) and chemical shifts of the Eu^{3+}-bound water protons from fitting of the PARACEST spectra using numerical solutions from modified Bloch equations and H4 protons from the high-resolution ^1H NMR spectra of the three complexes.[9]

	τ_m [μs] (calcd)[a]	δ [ppm][b]	δ [ppm][c]
Eu-**1**	200 ± 5	44.7	23.3
Eu-**2**	81 ± 1	54.0	26.1
Eu-**3**	55 ± 1	64.1	32.0

[a] Calculated Eu^{3+}-bound water lifetime. [b] Eu^{3+}-bound water chemical shift. [c] Eu^{3+}-macrocyclic H4 proton chemical shift.

Figure 1 shows individual CEST spectra for the three complexes at 298 K as well as a CEST spectrum of a mixture of the three complexes. The individual complexes showed three distinct exchange peaks for the Eu^{3+}-bound water protons at $\delta = 45$ ppm for Eu-**1**, $\delta = 54$ ppm for Eu-**2**, and $\delta = 64$ ppm for Eu-**3**, and even the CEST spectrum of the mixture showed relatively well-resolved exchange peaks for all three complexes (Figure S5d). As has been observed with other Eu^{3+}-based PARACEST agents, these complexes show decreased CEST sensitivities at 310 K, but the water exchange peaks in these complexes remain well-separated even at higher temperatures. The τ_m for each complex was determined by fitting modified Bloch equations to the PARACEST spectra using a non-linear fitting algorithm written in MATLAB (Table 1).[10] The magnitude of the H4 hyperfine shifts and Eu^{3+}-bound water chemical shifts are proportional to one another as expected, but one incidental finding was the inverse relationship between the magnitude of hyperfine shifts and the bound water lifetimes. This led to some preliminary computations on these systems to see if one could predict such relationships based on differences in metal ion–ligand interactions.

To gain a better understanding of the factors affecting the bound water exchange lifetimes in this series, the ligands were also examined using computational methods to quantify differences in their electronic properties. To simplify the calculations, one side-chain of each ligand was added to diethylamine to create fragments **1f**, **2f**, and **3f**—these were subsequently optimized using DFT calculations (B3LYP functional and 6-311G(d,p) basis set). The resulting Mulliken population analysis of the carbonyl oxygen and macrocyclic nitrogen was used to estimate the charge on each atom that coordinates to the Eu^{3+} ion (Table 2). The calculations

Table 2: Mulliken charges on the carbonyl oxygens in fragments **1f**, **2f**, and **3f**.

	1f	**2f**	**3f**
	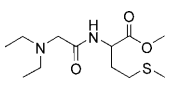	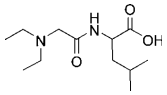	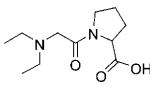
Mulliken charge	−0.491	−0.495	−0.517

showed that the negative charge on the carbonyl oxygen increases from **1f** < **2f** < **3f** while the charge on the nitrogen atoms in this series remains relatively constant (see Figures S10 and S11). This indicates that the oxygen donor atom in **3f** is a better electron donor than the oxygen atoms in either **2f** or **1f**, consistent with the measured water exchange rates for these three complexes, Eu-**3** > Eu-**2** > Eu-**1**. These data demonstrate that water exchange in these systems is quite sensitive to the amount of excess negative charge on the peptide carbonyl oxygen atom.

For simultaneous multi-frequency MR imaging, each agent must be activated ("turned on") by selective saturation of the bound water resonance in each complex without significant activation of the others. This was demonstrated in MR imaging experiments performed at 4.7 T by monitoring the bulk water signal using a standard spin–echo sequence preceded by selective presaturation on a six-well phantom (Figure 2a): water (W), Eu-**1**, Eu-**2**, Eu-**3**, and a mixture of the three complexes (M). The CEST images were obtained by subtracting the respective on-resonance frequency images from the off-resonance frequency images (Figure 2b) to eliminate any small intensity changes due to indirect saturation of the bulk water pool. As shown in the images and the corresponding graphs below each image (Figure 2c), application of a presaturation pulse at +45 ppm results in intense CEST contrast from Eu-**1** in the two wells that contained the compound (pure compound and the mixture). Under these experimental conditions, the well containing Eu-**2** showed about a 12% bleed-over effect while the well containing Eu-**3** showed no contrast. Similarly, application of a frequency-selective pulse at +55 ppm resulted in activation of Eu-**2**, 30% activation of Eu-**3**, and essentially no activation of Eu-**1**. Similar results were obtained when the saturation frequency was set to +65 ppm corresponding to activation of Eu-**3** in the presence of the others. From the graphical results (Figure 2c), it is clear that each complex shows greater than 70% selectivity in the presence of the other two agents using a B_1 of 9 μT. Of course, the degree of selectivity will depend upon the magnitude of the B_1 used to activate the agents; lower applied power levels will allow greater discrimination. For example, using a B_1 of 5 μT, one can readily discriminate all three agents with near 100% selectivity. A recent report showed that one can differentiate between the exchangeable NH protons of poly-L-arginine (PLR), poly-L-lysine (PLK) and the exchangeable OH protons of poly-L-threonine (PLT) using similar multi-frequency CEST imaging, even though the frequency range covered by these DIACEST agents is less than 3 ppm.[11] This was possible because proton exchange is considerably slower in the diamagnetic systems compared to water molecule exchange in the present Eu^{III}-DOTA-tetraamide systems, and this allows CEST activation using much lower applied B_1 fields (2.2 μT).

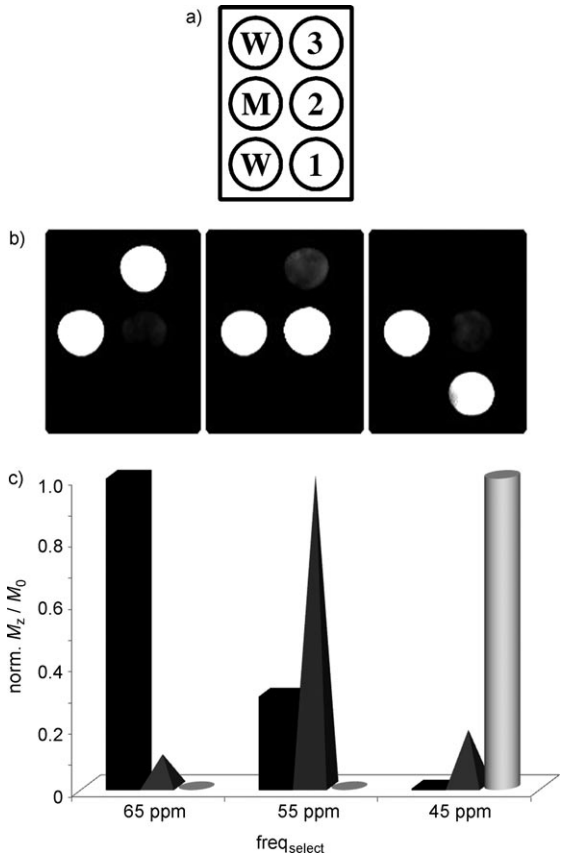

Figure 2. Phantom CEST images of the Eu^{3+} complexes Eu-**1** (20 mM), Eu-**2** (15 mM), and Eu-**3** (11 mM) recorded at 4.7 T, 298 K in water at pH 7 using a B_1 of 9 μT. a) Representation of the phantom containing six wells: water (W), Eu-**1**, Eu-**2**, Eu-**3**, and a mixture of the three complexes (M). b) PARACEST difference images of the complexes Eu-**1**, Eu-**2**, and Eu-**3**. c) Quantitative CEST contrast for each Eu^{3+} complex in the presence of other agents, Eu-**1** (cylinder), Eu-**2** (pyramid), and Eu-**3** (rectangle). Shown are the frequencies $freq_{select}$ at which the Eu^{III} complexes are selective.

In summary, we have demonstrated that Eu^{3+}-based paramagnetic complexes can be designed with relatively minor changes in the structure of the ligating arms to produce remarkably large differences in the resonance frequency of the bound water exchangeable protons. DFT calculations of the ligand side-chain fragments suggest a parallel between the negative charge on the carbonyl oxygen of each ligand and the corresponding water exchange rates and chemical shifts in the complexes. The three agents reported here span a frequency range of 20 ppm for the water exchange resonances, and this difference allows separate detection of each agent by CEST imaging. Given the fact that Eu^{III}-DOTA-tetraamide complexes tend to exhibit the slowest water exchange kinetics among all other Ln^{3+} ion complexes, the possibility of even greater chemical diversity in the ligand side-chains compared to those reported here may offer an opportunity to create a palette of multi-frequency Eu^{3+}-based PARACEST agents.

Experimental Section

CEST imaging was performed on a phantom of 3×2 wells. Images were acquired on a Varian INOVA 4.7 T horizontal animal MR imaging system. A spin–echo sequence was preceded by a presaturation pulse of fixed frequency at three different on-resonance frequencies of +45 ppm, +54 ppm and +64 ppm and their corresponding off-resonance frequencies. Resolution = 128×128; field of view (FOV) 25×25 mm; repetition time (TR) 10 s; echo time (TE) 13 ms; dummy scans 4; saturation power 9 μT; irradiation time 4 s. Image processing was performed using ImageJ (NIH).

The synthetic details for preparation of the ligands and complexes, CEST spectra of the Eu^{3+} complexes as a function of applied B_1, CEST fitting procedures, and the protocol for DFT calculations are available in the Supporting Information.

Received: August 20, 2009
Published online: November 5, 2009

Keywords: europium · imaging agents · macrocycles · PARACEST · saturation transfer

[1] K. M. Ward, A. H. Aletras, R. S. Balaban, *J. Magn. Reson.* **2000**, *143*, 79.
[2] S. Zhang, P. Winter, K. Wu, A. D. Sherry, *J. Am. Chem. Soc.* **2001**, *123*, 1517.
[3] S. Zhang, M. Merritt, D. E. Woessner, R. E. Lenkinski, A. D. Sherry, *Acc. Chem. Res.* **2003**, *36*, 783.
[4] S. Aime, C. Carrera, D. Delli Castelli, S. Geninatti Crich, E. Terreno, *Angew. Chem.* **2005**, *117*, 1847; *Angew. Chem. Int. Ed.* **2005**, *44*, 1813.
[5] a) S. Aime, A. Barge, D. D. Castelli, F. Fedeli, A. Mortillaro, F. U. Nielsen, E. Terreno, *Magn. Reson. Med.* **2002**, *47*, 639; b) S. Zhang, C. R. Malloy, A. D. Sherry, *J. Am. Chem. Soc.* **2005**, *127*, 17572; c) S. J. Ratnakar, M. Woods, A. J. M. Lubag, Z. Kovacs, A. D. Sherry, *J. Am. Chem. Soc.* **2008**, *130*, 6; d) S. Aime, D. Delli Castelli, F. Fedeli, E. Terreno, *J. Am. Chem. Soc.* **2002**, *124*, 9364; e) S. Zhang, R. Trokowski, A. D. Sherry, *J. Am. Chem. Soc.* **2003**, *125*, 15288.
[6] a) M. Woods, D. E. Woessner, A. D. Sherry, *Chem. Soc. Rev.* **2006**, *35*, 500; b) F. Wojciechowski, M. Suchy, A. X. Li, H. A. Azab, R. Bartha, R. H. E. Hudson, *Bioconjugate Chem.* **2007**, *18*, 1625.
[7] a) T. Mani, G. Tircso, O. Togao, P. Zhao, T. C. Soesbe, M. Takahashi, A. D. Sherry, *Contrast Media Mol. Imaging* **2009**, *4*, 183; b) S. Zhang, X. Jiang, A. D. Sherry, *Helv. Chim. Acta* **2005**, *88*, 923.
[8] L. M. De León-Rodríguez, S. Viswanathan, A. D. Sherry, *Contrast Media Mol. Imaging* **2009**, submitted.
[9] S. Zhang, Z. Kovacs, S. Burgess, S. Aime, E. Terreno, A. D. Sherry, *Chem. Eur. J.* **2001**, *7*, 288.
[10] D. E. Woessner, S. Zhang, M. E. Merritt, A. D. Sherry, *Magn. Reson. Med.* **2005**, *53*, 790.
[11] M. T. McMahon, A. A. Gilad, M. A. DeLiso, S. M. C. Berman, J. W. M. Bulte, P. C. M. van Zijl, *Magn. Reson. Med.* **2008**, *60*, 803.

